

1           Recent Northern Hemisphere stratospheric HCl increase  
2                           due to atmospheric circulation changes

3           E. Mahieu<sup>1</sup>, M.P. Chipperfield<sup>2</sup>, J. Notholt<sup>3</sup>, T. Reddmann<sup>4</sup>, J. Anderson<sup>5</sup>,  
4           P.F. Bernath<sup>6,7,8</sup>, T. Blumenstock<sup>4</sup>, M.T. Coffey<sup>9</sup>, S.S. Dhomse<sup>2</sup>, W. Feng<sup>2</sup>, B. Franco<sup>1</sup>,  
5           L. Froidevaux<sup>10</sup>, D.W.T. Griffith<sup>11</sup>, J.W. Hannigan<sup>9</sup>, F. Hase<sup>4</sup>, R. Hossaini<sup>2</sup>, N.B. Jones<sup>11</sup>,  
6           I. Morino<sup>12</sup>, I. Murata<sup>13</sup>, H. Nakajima<sup>12</sup>, M. Palm<sup>3</sup>, C. Paton-Walsh<sup>11</sup>,  
7           J.M. Russell III<sup>5</sup>, M. Schneider<sup>4</sup>, C. Servais<sup>1</sup>, D. Smale<sup>14</sup>, K.A. Walker<sup>8,15</sup>

8

9           **Affiliations**

- 10           1. Institute of Astrophysics and Geophysics, University of Liège, Liège 4000,  
11           Belgium
- 12           2. National Centre for Atmospheric Science, School of Earth and Environment,  
13           University of Leeds, Leeds, LS2 9JT, U.K.
- 14           3. Department of Physics, University of Bremen, Bremen 28334, Germany
- 15           4. Karlsruhe Institute of Technology (KIT), Institute for Meteorology and Climate  
16           Research (IMK-ASF), Karlsruhe 76021, Germany
- 17           5. Department of Atmospheric and Planetary Science, Hampton University,  
18           Hampton, Virginia 23668, USA
- 19           6. Department of Chemistry & Biochemistry, Old Dominion University, Norfolk,  
20           Virginia 23529, USA
- 21           7. Department of Chemistry, University of York, York, YO10 5DD, U.K.
- 22           8. Department of Chemistry, University of Waterloo, Waterloo, Ontario, N2L 3G1,  
23           Canada
- 24           9. National Center for Atmospheric Research, Boulder, Colorado 80307, USA
- 25           10. Jet Propulsion Laboratory, California Institute of Technology, Pasadena,  
26           California 91109, USA
- 27           11. School of Chemistry, University of Wollongong, Wollongong, New South Wales  
28           2522, Australia
- 29           12. National Institute for Environmental Studies (NIES), Tsukuba, Ibaraki 305-8506,  
30           Japan

- 31 13. Graduate School of Environmental Studies, Tohoku University, Sendai 980-8578,  
32 Japan
- 33 14. National Institute of Water and Atmospheric Research (NIWA), Lauder 9352,  
34 New Zealand
- 35 15. Department of Physics, University of Toronto, Toronto, Ontario, M5S 1A7,  
36 Canada
- 37

38 The abundance of chlorine in the Earth's atmosphere increased considerably during  
39 the 1970s to 1990s, following large emissions of anthropogenic long-lived chlorine-  
40 containing source gases, notably the chlorofluorocarbons. The chemical inertness of  
41 chlorofluorocarbons allows their transport and mixing throughout the troposphere  
42 on a global scale<sup>1</sup>, before they reach the stratosphere where they release chlorine  
43 atoms that cause ozone depletion<sup>2</sup>. The large ozone loss over Antarctica<sup>3</sup> was the key  
44 observation which stimulated the definition and signing in 1987 of the Montreal  
45 Protocol, an international treaty establishing a schedule to reduce the production of  
46 the major chlorine- and bromine-containing halocarbons. Owing to its  
47 implementation, the near-surface total chlorine concentration showed a maximum  
48 in 1993, followed by a decrease of half a per cent to one per cent per year<sup>4</sup>, in line  
49 with expectations. Remote-sensing data have revealed a peak in stratospheric  
50 chlorine after 1996<sup>5</sup>, then a decrease at rates close to one per cent per year<sup>6,7</sup>, in  
51 agreement with the surface observations of the chlorine source gases and model  
52 calculations<sup>7</sup>. Here we present ground-based and satellite data which show a recent  
53 and significant increase, at the  $2\sigma$  level, in hydrogen chloride (HCl), the main  
54 stratospheric chlorine reservoir, starting around 2007 in the Northern Hemisphere  
55 lower stratosphere, contrasting with the ongoing monotonic decrease of near-  
56 surface source gases. Using model simulations we attribute this trend anomaly to a  
57 slowdown in the Northern Hemisphere atmospheric circulation, occurring over  
58 several consecutive years, transporting more aged air to the lower stratosphere, and  
59 characterized by a larger relative conversion of source gases to HCl. This short-term

60 **dynamical variability will also affect other stratospheric tracers and needs to be**  
61 **accounted for when studying the evolution of the stratospheric ozone layer.**

62 Decomposition of chlorine-containing source gases in the stratosphere produces HCl, the  
63 largest reservoir of chlorine<sup>8,9</sup>. Here we investigate recent trends in atmospheric HCl  
64 using observations from eight Network for the Detection of Atmospheric Composition  
65 Change (NDACC; <http://www.ndacc.org>) ground-based stations located between 79°N –  
66 45°S and operating Fourier Transform InfraRed (FTIR) instruments. Figure 1a shows the  
67 HCl total columns for Jungfraujoch (47°N; red squares) together with the evolution of the  
68 total tropospheric chlorine (blue curve) over the past three decades. Figure 1b-d focuses  
69 on the recent HCl changes above Ny-Ålesund (79°N) and two mid-latitude stations,  
70 Jungfraujoch (zoom of Fig 1a) and Lauder (45°S).

71 At the southern hemisphere station we find a continuous decrease of HCl since 2001, but  
72 both Northern Hemisphere sites show an overall HCl decline, more rapid around 2004,  
73 followed by an increase from 2007 onwards. To quantify the column changes at all sites,  
74 we used a bootstrap resampling statistical tool<sup>10</sup> involving a linear component and  
75 accounting for the strong seasonal modulations present in the data sets. Figure 2 displays  
76 for the eight NDACC sites the relative annual HCl rates of change for the 1997–2007 and  
77 2007–2011 time periods, using either the 1997.0 or 2007.0 computed column as  
78 reference. For the 1997-2007 time interval, we determine consistent and significant HCl  
79 decreases at all Northern Hemisphere sites, with mean relative changes ranging from –0.7  
80 to –1.5 per cent per year. In the Southern Hemisphere, column changes are not significant  
81 at the  $2\sigma$  level. For 2007-2011, mean relative column growths of 1.1–3.4 per cent per year

82 are derived for all Northern Hemisphere sites while negative or undefined rates are  
83 observed for Wollongong and Lauder in the Southern Hemisphere.

84 To corroborate these findings with independent data, and to get information on the  
85 altitude range where these changes occur, we included the GOZCARDS<sup>11</sup> satellite data  
86 set (Global OZone Chemistry And Related Datasets for the Stratosphere version1.01),  
87 which merges observations by the HALOE<sup>12</sup> (HALogen Occultation Experiment version  
88 19), ACE-FTS<sup>13</sup> (Atmospheric Chemistry Experiment-Fourier Transform Spectrometer  
89 version 2.2) and Aura/MLS<sup>14</sup> (Microwave Limb Sounder version 3.3) instruments. Partial  
90 columns were computed between 100 hPa and 10 hPa, considering the zonal monthly  
91 mean mixing ratio time series available for the whole time interval in the 70°–80°N, 60°–  
92 70°N, 40°–50°N, 30°–40°N, 20°–30°N, 30°–40°S and 40°–50°S latitudinal bands. These  
93 partial columns typically span altitudes of 16–31 km, that is, the region with maximum  
94 HCl concentration and in which the FTIR measurements are most sensitive<sup>5</sup>.  
95 Corresponding rates of change are also displayed in Fig. 2. For 1997–2007, there is  
96 excellent agreement in the Northern Hemisphere between the satellite and the six  
97 NDACC-FTIR trends determined above. In the Southern Hemisphere, GOZCARDS  
98 reveals statistically significant decreases of HCl at the  $2\sigma$  level, while the FTIR time series  
99 suggest stable columns at the same level of confidence. For 2007–2011, the ACE-FTS  
100 and Aura/MLS merged data confirm the upward FTIR trends in the northern hemisphere.  
101 Figure 3 illustrates this, showing satellite monthly means (red dots) for 30°–60°N and  
102 30°–60°S, at 46 hPa and 7 hPa, together with a linear fit to the data for both time periods.  
103 The HCl increase is clearly confined to the Northern Hemisphere lower stratosphere.

104 Because HCl is the main final product of the decomposition of any chlorine-containing  
105 source gases, we need to verify that its rise after 2007 does not result from the substantial  
106 contribution of new unknown sources of chlorine whose emissions occur predominantly  
107 in the Northern Hemisphere, not monitored by the *in situ* networks, and unregulated by  
108 the Montreal Protocol, its Amendments and Adjustments. Indeed, such chlorine-  
109 containing source gases have been recently identified<sup>15</sup> although in that case, their  
110 contribution to the HCl upturn can be ruled out by their very low concentrations.

111 We have used results from two state-of-the-art three-dimensional chemical transport  
112 models, SLIMCAT<sup>7</sup> and KASIMA<sup>7</sup>, to interpret the recent HCl increase. Both models  
113 performed a standard simulation using surface source gas mixing ratios from the WMO  
114 A1 (World Meteorological Organisation; 2010) emission scenario<sup>4</sup> and were forced using  
115 ERA-Interim meteorological fields<sup>16</sup> from the European Centre for Medium-Range  
116 Weather Forecasts (ECMWF). The key results for HCl trends from both models agree.  
117 Here we show data from the SLIMCAT runs; corresponding results from KASIMA are  
118 shown in the Extended Data Figs 1–4. To study the impact of atmospheric dynamics, an  
119 additional SLIMCAT run (S2000) used constant 2000 meteorological forcing, from 2000  
120 onwards.

121 Running averages for both SLIMCAT simulations are reproduced in Fig. 1b–d. For the  
122 three sites, run S2000 (light green curve) predicts an overall HCl decrease while the  
123 standard run (green squares) reproduces the observed and distinct evolution prevailing in  
124 both hemispheres, after correction of a constant low-bias of about 7% in the Northern  
125 Hemisphere simulations. The total column changes characterizing the model data sets are

126 displayed in Fig. 2. The model runs predict significant decreases in HCl for the 1997–  
127 2007 reference period at all sites and there is an overall agreement within the error bars  
128 for the amplitude of the signals between the model and the observations. Regarding the  
129 2007–2011 time period, the SLIMCAT time series are characterized by positive trends  
130 from Ny-Ålesund (79°N) to Tsukuba (36°N), and by significant decreases for the  
131 Southern Hemisphere stations, but show no change for the near-tropical site of Izana  
132 (28°N). The S2000 sensitivity run does not produce the HCl trend reversal and, instead,  
133 indicates declines at all sites.

134 The agreement between measurement and model demonstrates that the HCl increase after  
135 2007 is not caused by new, unidentified chlorine sources, or by underestimates in  
136 emissions of known species of chlorine-containing source gases, because these are used  
137 as model input. The agreement between model and observation also shows that there is a  
138 good understanding of the chemistry which converts source gases to HCl. The difference  
139 between the HCl trends forecasted by the two SLIMCAT runs—that is, a significant  
140 increase for northern high- and mid-latitudes or a constant decrease below 30°N—  
141 establishes that changes in the atmospheric circulation cause the recent HCl increase,  
142 since only the meteorological fields adopted from 2000 onwards differ between the two  
143 runs. To diagnose these circulation changes, we examined age-of-air maps produced by  
144 the standard SLIMCAT run. They reveal a slower circulation in the Northern Hemisphere  
145 lower stratosphere after 2005–2006, with older air characterized by a larger relative  
146 conversion of the chlorine-containing source gases into HCl.

147 Figure 4b shows the age-of-air change between 2005–2006 and 2010–2011. Air older by  
148 up to 0.4 yr is found around 20–25 km altitude in a broad range of Northern Hemisphere  
149 latitudes, in a region where the mean age-of-air is typically about 3 yr. There is an  
150 obvious correlation with the evolution of the HCl concentrations over the same time  
151 period (Fig 4a) which exhibits a very similar pattern and hemispheric asymmetry. Time  
152 series of mean age-of-air near 50 hPa above Ny-Ålesund, Jungfrauoch and Lauder are  
153 displayed in Fig.4c. The 3-yr running means (black curves) indicate a progressive  
154 slowdown of the Northern Hemisphere stratospheric circulation after 2005–2006. For  
155 Lauder, a fairly constant circulation speedup occurs from 2000 onwards.

156 These changes are significant at the  $2\sigma$  level, with Northern Hemisphere air ageing by 3–4  
157 weeks per year after 2005, compared to about 1 week per year before. For Lauder, the  
158 mean age-of-air change during the last decade is calculated to be –2 weeks per year.  
159 Other important factors such as the details of specific transport pathways, which lead to a  
160 given mean age-of-air, also affect the conversion rate of the source gases to HCl (ref. 17).  
161 These pathways are simulated by the model but not revealed by the simple diagnostic of  
162 mean age-of-air. The slower Northern Hemisphere circulation occurring over a few years  
163 after 2005–2006 seems to contrast with the speedup of the Brewer–Dobson circulation  
164 which is predicted in the very long-term to be a response to climate change<sup>18,19</sup>, but the  
165 recent slowdown is likely part of dynamical variability occurring on shorter timescales: it  
166 does not imply a change in the general circulation strength. More than year-to-year  
167 variability, it is multiyear periods of age-of-air increase or decrease, such as those  
168 highlighted in our study or reported recently<sup>20</sup>, that will probably complicate the search of  
169 a long-term trend in mean circulation.



170 We have presented observations and simulations of a recent HCl increase in the Northern  
171 Hemisphere lower stratosphere. We ascribe it to dynamical variability, occurring on a  
172 timescale of a few years, characterized by a persistent slowing of stratospheric circulation  
173 after 2005, bringing HCl-enriched air into the Northern Hemisphere lower stratosphere.  
174 We find no evidence that unidentified chlorine-containing source gases are responsible  
175 for this HCl increase. In the Southern Hemisphere, a fairly constant decrease has been  
176 observed over the past ten years. Globally, our ground-based observations indicate a  
177 mean HCl decrease of 0.5 per cent per year for 1997–2011, compatible with the 0.5–1 per  
178 cent per year range that characterized the post-peak reduction of tropospheric chlorine<sup>4</sup>.  
179 Hence, we conclude that the Montreal Protocol is still on track, and is leading to an  
180 overall reduction of the stratospheric chlorine loading. However, multiyear variability in  
181 the stratospheric circulation and dynamics, as identified here, could lead to further  
182 unpredictable increases or redistribution of HCl and other stratospheric tracers.  
183 Therefore, such variability and its causes will have to be thoroughly characterized and  
184 carefully accounted for when evaluating trends or searching for ozone recovery.  
185

186 **References**

- 187 1. Lovelock, J. E., Maggs, R. J., and Wade, R. J. Halogenated hydrocarbons in and over  
188 the Atlantic. *Nature* **241**, 194–196 (1973).
- 189 2. Molina, M. J. and Rowland, F. S. Stratospheric sink for chlorofluoromethanes:  
190 chlorine atom-catalysed destruction of ozone. *Nature* **249**, 810–812 (1974).
- 191 3. Farman, J. C., Gardiner, B. G., and Shanklin, J. D. Large losses of total ozone in  
192 Antarctica reveal seasonal ClO<sub>x</sub>/NO<sub>x</sub> interaction. *Nature* **315**, 207–210 (1985).
- 193 4. World Meteorological Organization. *Scientific Assessment of Ozone Depletion: 2010*  
194 (Report 52, Global Ozone Research and Monitoring Project, 2011).
- 195 5. Rinsland, C. P. *et al.* Long-term trends of inorganic chlorine from ground-based  
196 infrared solar spectra: Past increases and evidence for stabilization. *J. Geophys. Res.*  
197 **108**, 24235–24249 (2003).
- 198 6. Froidevaux, L., *et al.* Temporal decrease in upper atmospheric chlorine. *Geophys.*  
199 *Res. Lett.* **33**, doi:10.1029/2006GL027600 (2006).
- 200 7. Kohlhepp, R. *et al.* Observed and simulated time evolution of HCl, ClONO<sub>2</sub>, and HF  
201 total column abundances. *Atmos. Chem. Phys.* **12**, 3527–3557 (2012).
- 202 8. Zander, R. *et al.* The 1985 chlorine and fluorine inventories in the stratosphere based  
203 on ATMOS observations at 30° north latitudes. *J. Atmos. Chem.* **15**, 171–186 (1992).
- 204 9. Nassar, R. *et al.* A global inventory of stratospheric chlorine in 2004. *J. Geophys. Res.*  
205 **111**, D22312 doi:10.1029/2006JD007073 (2006).
- 206 10. Gardiner, T. *et al.* Trend analysis of greenhouse gases over Europe measured by a  
207 network of ground-based remote FTIR instruments. *Atmos. Chem. Phys.* **8**, 6719–  
208 6727 (2008).

- 209 11. Froidevaux, L. *et al.* GOZCARDS Merged Data for Hydrogen Chloride Monthly  
210 Zonal Means on a Geodetic Latitude and Pressure Grid, version 1.01,  
211 <http://dx.doi.org/10.5067/MEASURES/GOZCARDS/DATA3002> (NASA Goddard  
212 Earth Science Data and Information Services Center, accessed June, 2013).
- 213 12. Russell, J. M., III, *et al.* The Halogen Occultation Experiment. *J. Geophys. Res.* **98**,  
214 10777–10797 (1993).
- 215 13. Bernath, P. F. *et al.* Atmospheric Chemistry Experiment (ACE): mission overview.  
216 *Geophys. Res. Lett.* **32**, doi:10.1029/2005GL022386 (2005).
- 217 14. Waters, J. W. *et al.* The Earth Observing System Microwave Limb Sounder (EOS  
218 MLS) on the Aura satellite. *IEEE Trans. Geosci. Remote Sens.* **44**, 1075–1092 (2006).
- 219 15. Laube, J. C. *et al.* Newly detected ozone-depleting substances in the atmosphere.  
220 *Nature Geoscience*, doi:10.1038/ngeo2109 (2014).
- 221 16. Dee, D. P. *et al.* The ERA-Interim reanalysis: configuration and performance of the  
222 data assimilation system. *Q. J. Roy. Meteorol. Soc.* **137**, 553–597 (2011).
- 223 17. Waugh, D. W., Strahan, S. E., and Newman, P. A. Sensitivity of stratospheric  
224 inorganic chlorine to differences in transport. *Atmos. Chem. Phys.* **7**, 4935–4941  
225 (2007).
- 226 18. Engel, A. *et al.* Age of stratospheric air unchanged within uncertainties over the past  
227 30 years. *Nature Geoscience* **2**, 28–31 (2009).
- 228 19. McLandress, C. and Shepherd, T.G. Simulated anthropogenic changes in the Brewer-  
229 Dobson circulation, including its extension to high latitude. *J. Climate* **22**, 1516–  
230 1540, (2009).

231 20. Stiller, G. P., *et al.* Observed temporal evolution of global mean age of stratospheric  
232 air for the 2002 to 2010 period. *Atmos. Chem. Phys.* **12**, 3311–3331 (2012).

233 21. Rothmann, L. S. *et al.* The HITRAN 2008 molecular spectroscopic database. *J.*  
234 *Quant. Spec. and Rad. Transf.* **110**, 533–572 (2009).

### 235 **Acknowledgments**

236 The University of Liège contribution was mainly supported by the Belgian Science  
237 Policy Office (BELSPO) and the Fonds de la Recherche Scientifique – FNRS, both in  
238 Brussels. Additional support was provided by MeteoSwiss (Global Atmospheric Watch)  
239 and the Fédération Wallonie–Bruxelles. We thank the International Foundation High  
240 Altitude Research Stations Jungfrauoch and Gornergrat (HFSJG, Bern). We thank O.  
241 Flock and D. Zander (University of Liège). The SLIMCAT modelling work was  
242 supported by the UK Natural Environment Research Council (NCAS and NCEO). The  
243 FTIR measurements at Ny-Ålesund, Spitsbergen, are supported by the AWI  
244 Bremerhaven. The work from Hampton University was partially funded under the NASA  
245 MEASURE’s GOZCARDS program and the National Oceanic and Atmospheric  
246 Administration’s Educational Partnership Program Cooperative Remote Sensing Science  
247 and Technology Center (NOAA EPP CREST). The ACE mission is supported primarily  
248 by the Canadian Space Agency. We thank U. Raffalski and P. Voelger for technical  
249 support at IRF Kiruna. The National Center for Atmospheric Research is supported by  
250 the National Science Foundation. The observation program at Thule, Greenland is  
251 supported under contract by the National Aeronautics and Space Administration (NASA)  
252 and the site is also supported by the NSF Office of Polar Programs. We thank the Danish  
253 Meteorological Institute for support at the Thule. Work at the Jet Propulsion Laboratory,

254 California Institute of Technology, was performed under contract with NASA; the  
255 assistance of R. Fuller in producing the GOZCARDS data set is acknowledged, and work  
256 by many ACE-FTS, HALOE, and MLS team members who helped to produce data  
257 towards the GOZCARDS data set is also acknowledged. We thank O. E. García, E.  
258 Sepúlveda, and the State Meteorological Agency (AEMET) of Spain for scientific and  
259 technical support at Izana. The Australian Research Council has provided significant  
260 support over the years for the NDACC site at Wollongong, most recently as part of  
261 project DP110101948. Measurements at Lauder are core funded through New Zealand's  
262 Ministry of Business, Innovation and Employment. We are grateful to all colleagues who  
263 have contributed to FTIR data acquisition. We thank ECMWF for providing the ERA-  
264 Interim reanalyses.

#### 265 **Author contributions**

266 MP, JWH, FH, EM, I. Mu., NBJ and CPW, DS performed the Ny-Ålesund, Thule,  
267 Kiruna and Izana, Jungfraujoch, Tsukuba, Wollongong and Lauder retrievals for HCl,  
268 respectively. PFB and KAW provided ACE-FTS data, LF and JA the GOZCARDS  
269 dataset. JA, PFB, LF, JMR III and KAW provided expertise on satellite data usage. MPC,  
270 RH, SSD and WF designed and performed the SLIMCAT runs, sensitivity analyses and  
271 transport diagnostics. TR performed the KASIMA model run and corresponding  
272 diagnostics. BF and EM performed the trend analyses and compiled the results. JN, MTC,  
273 TB, CS, I. Mo. and HN, MS, DWTG and DS are responsible for the instrumentation and  
274 data acquisition at the NDACC stations. EM initiated and coordinated the study. The  
275 figures were prepared by EM and BF (Fig. 1), EM (Fig. 2), RH and MPC (Fig. 3) and TR

276 (Fig. 4). EM, MPC and JN wrote the manuscript. Together with TR, they revised it and

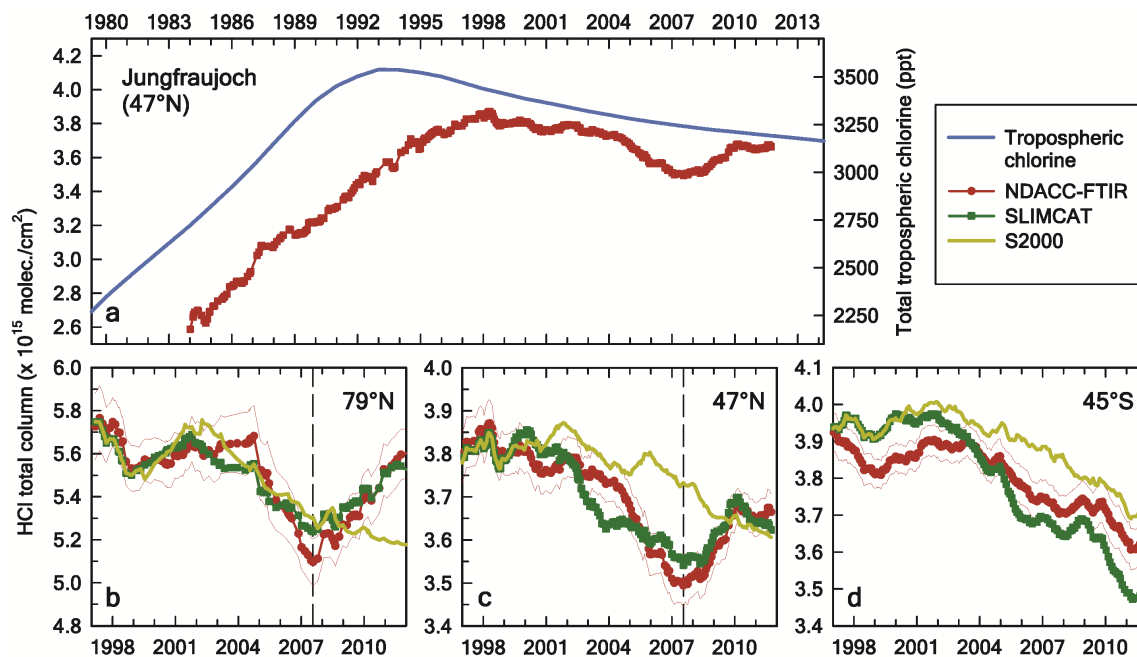
277 included the comments from the co-authors.

278

279 **Author information**

280 Reprints and permissions information is available at [www.nature.com/reprints](http://www.nature.com/reprints). The  
281 authors declare no competing financial interests. Readers are welcome to comment on the  
282 online version of the paper. Correspondence and requests for materials should be  
283 addressed to E.M. ([emmanuel.mahieu@ulg.ac.be](mailto:emmanuel.mahieu@ulg.ac.be)). NDACC data are publicly available at  
284 <ftp://ftp.cpc.ncep.noaa.gov/ndacc/station/> and GOZCARDS data are publicly available at  
285 <http://measures.gsfc.nasa.gov/opendap/GOZCARDS/>.

286



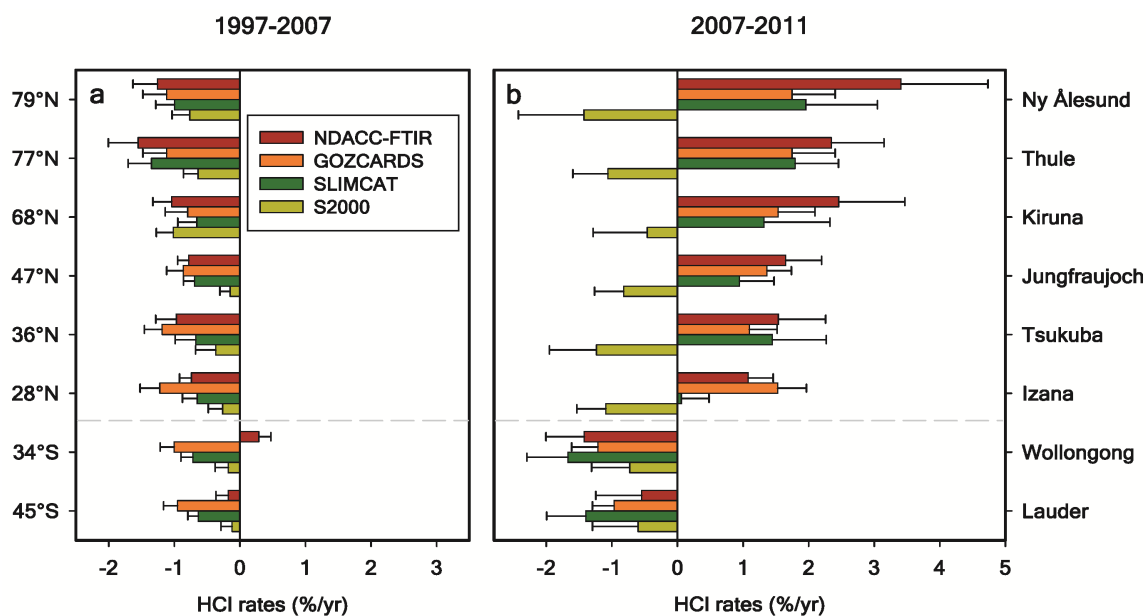
287

288 **Figure 1 | Evolution of hydrogen chloride (HCl) in the Earth's atmosphere. a,** The  
 289 long-term total column time series of HCl at Jungfraujoch (running average with a 3-yr  
 290 integration length, step of 1 month; in red, left scale) and the global total tropospheric  
 291 chlorine volume mixing ratio (blue curve, right scale, in parts per trillion, p.p.t.). The  
 292 lower panels display the running average total column time series (1997–2011) of HCl at  
 293 Ny-Ålesund (b), Jungfraujoch (c) and Lauder (d), derived from the NDACC–FTIR  
 294 observations, and the standard (green) and S2000 (light green) SLIMCAT simulations.  
 295 The thin red lines correspond to the  $\pm 2$  standard error of the mean range. Minimum  
 296 columns are observed in July 2007 at the Northern Hemisphere sites (dashed lines).

297



298

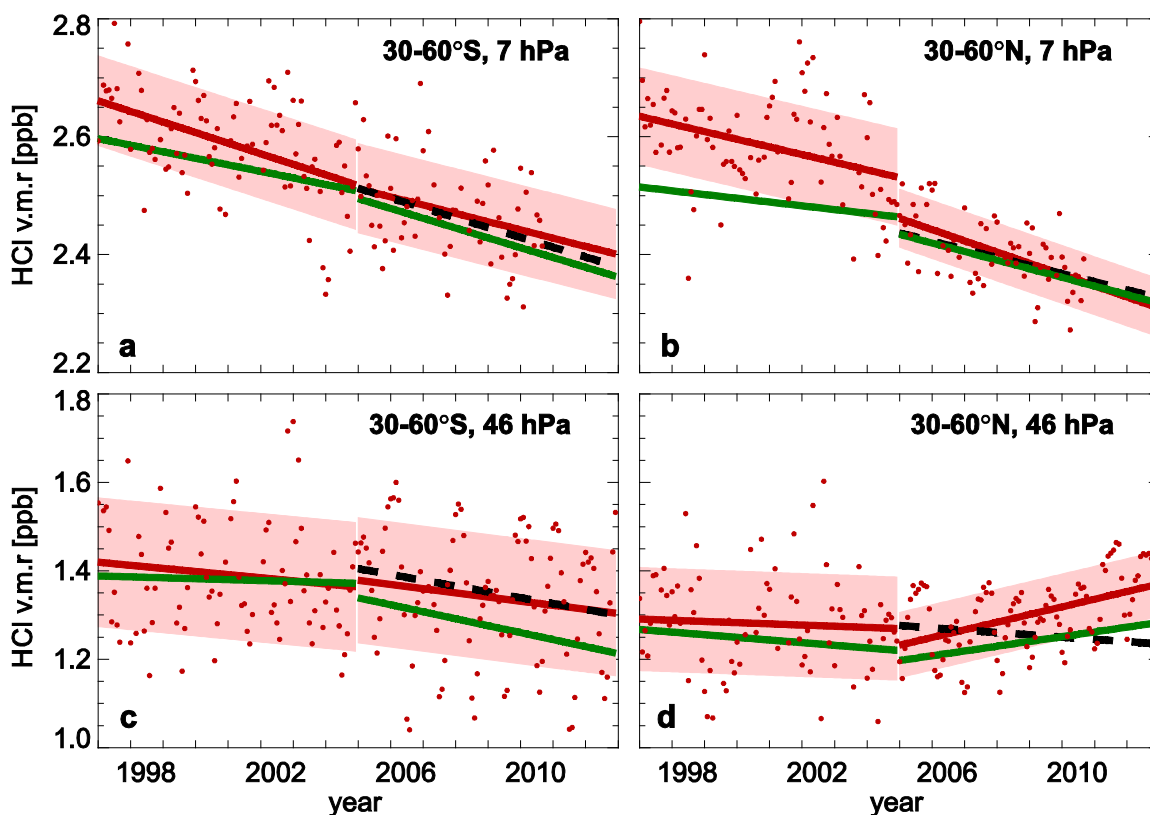


299

300 **Figure 2 | HCl relative rates of change for eight NDACC sites. a,** The rates of change  
301 (per cent per year) for the 1997–2007 time period (1999–2007 for Thule and Izana, 1998–  
302 2007 for Tsukuba). **b,** As for **a** but for 2007–2011. The rates of change were derived from  
303 the FTIR and GOZCARDS observational data sets and from the two SLIMCAT  
304 simulated time series (see colour key). The error bars correspond to the  $2\sigma$  level of  
305 uncertainty.

306

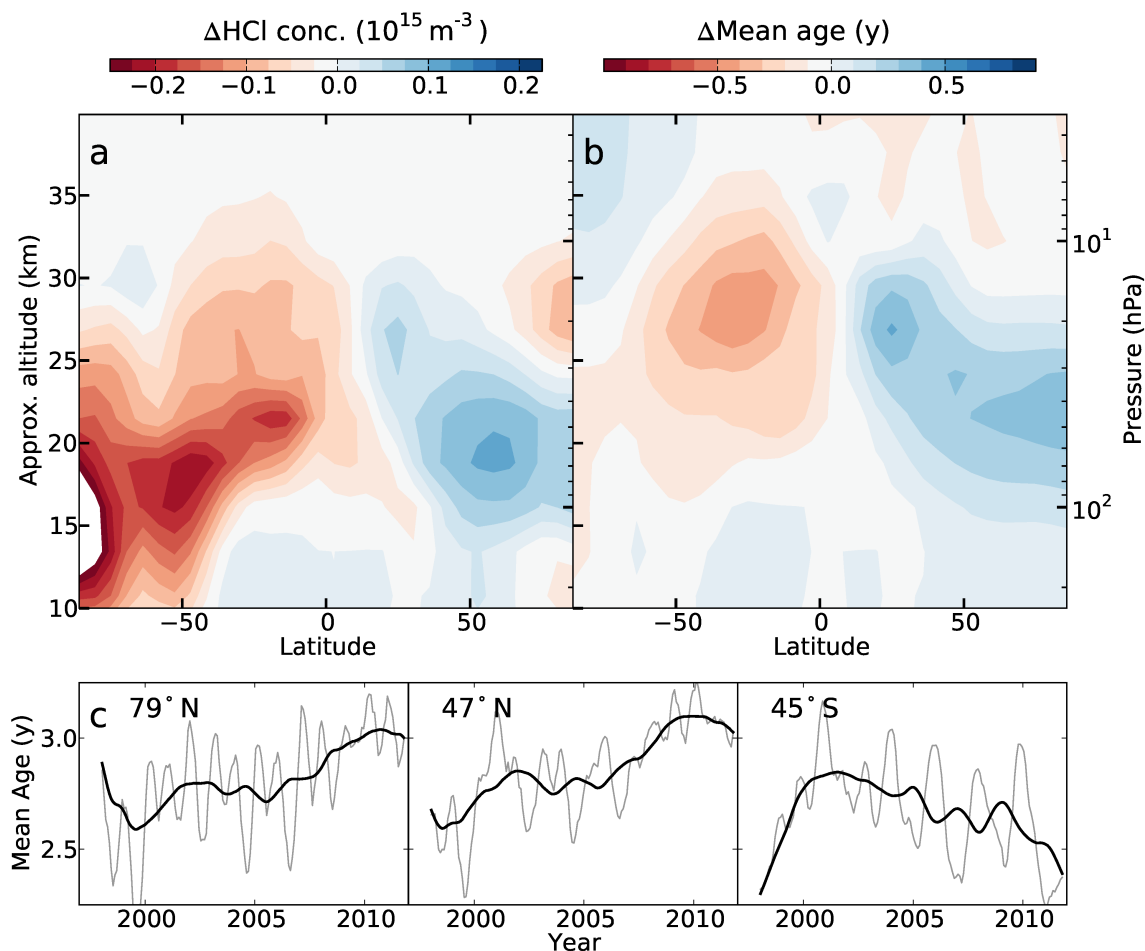
307



308

309 **Figure 3 | Evolution of stratospheric HCl from satellite observations.** Comparison of  
310 merged GOZCARDS satellite HCl observations (by HALOE, ACE-FTS and Aura/MLS)  
311 with SLIMCAT model runs for Northern Hemisphere and Southern Hemisphere mid-  
312 latitude lower (46 hPa) and upper (7 hPa) stratosphere. GOZCARDS monthly means are  
313 shown as red dots. Linear fits to the GOZCARDS data and standard SLIMCAT run are  
314 displayed as red and green lines, respectively, for periods before and after 2005. The  
315 dashed black line shows fits to the S2000 run, which assumes no change in circulation.  
316 An upward trend is observed in the Northern Hemisphere lower stratosphere (**d**) while  
317 HCl is decreasing in the southern and northern upper stratosphere (**a**, **b**); volume mixing  
318 ratio (vmr) in parts per billion (p.p.b.).

319



320

321 **Figure 4 | Spatial distribution of the HCl concentration and age-of-air changes.**

322 Mean differences of the HCl concentration (a) and age-of-air (b) between 2010/2011 and

323 2005/2006, as a function of altitude and latitude, derived from the standard SLIMCAT

324 simulation. There is a clear asymmetry between the hemispheres, with correlated patterns

325 between age-of-air and HCl, indicating that the HCl changes over that period are

326 consistent with slower/faster circulation in the Northern/Southern Hemisphere. c,

327 Running averages of the mean age-of-air at 50 hPa (thick/thin curve, integration length of

328 36/6 months), at the same sites as Fig. 1 (time series at 79°N and 45°S have been shifted

329 vertically by  $-0.75$  yr).

330

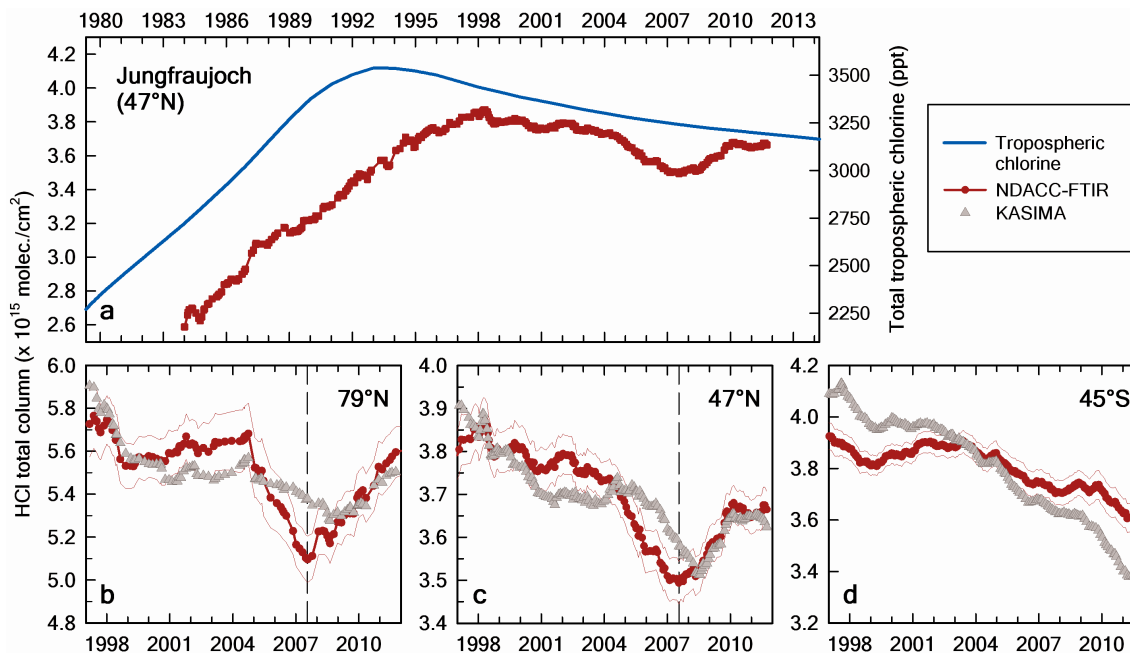
331 **Methods**

332 The ground-based observations were performed at the NDACC sites by solar absorption  
333 spectrometry in the infrared spectral region, using FTIR high-resolution instruments.  
334 Observations are recorded under clear sky conditions year-round, except at Ny-Ålesund  
335 and Thule, where the polar night prevents measurements between about October and  
336 February. The HCl total columns were retrieved with the SFIT-2, SFIT-4 or PROFFIT  
337 algorithm in narrow spectral ranges encompassing isolated lines of HCl<sup>5,7</sup>, generally  
338 assuming pressure-temperature profiles provided by the National Centers for  
339 Environmental Prediction (NCEP). The GOZCARDS<sup>11</sup> dataset for HCl includes zonal  
340 average monthly mean time series of stratospheric mixing ratio profiles merging  
341 individual measurements from the HALOE (1991–2005), ACE-FTS (2004 onward) and  
342 Aura MLS (2004 onward) satellite-borne instruments. Line parameters from recent  
343 HITRAN databases<sup>21</sup> were adopted in the spectrometric analyses. We used the  
344 SLIMCAT and KASIMA models<sup>7</sup> to support our investigations. Both used ERA-Interim  
345 analyses provided by ECMWF<sup>16</sup>, and they provided consistent results for the HCl trends,  
346 giving confidence in their robustness. The models contain detailed treatments of  
347 stratospheric chemistry and have been extensively used for studies of stratospheric  
348 ozone<sup>7</sup>. Stratospheric age-of-air was diagnosed in the model runs using an idealised tracer  
349 with a linearly increasing tropospheric mixing ratio. For the S2000 SLIMCAT  
350 simulation, 6-hourly winds of 2000 were used every year from 2000 onwards. The trend  
351 determinations were performed with a bootstrap resampling statistical tool<sup>10</sup>, considering all  
352 available daily or monthly means (excluding the winter months for the very high-latitude  
353 sites) while the model datasets were limited to days with available FTIR measurements. We

354 studied the impact of the FTIR sampling using the bootstrap algorithm, and found no

355 statistically significant impact on the calculated trends.

356



357

358 **Extended Data Figure 1 | Evolution of hydrogen chloride (HCl) in the Earth's**359 **atmosphere and comparison with KASIMA model results. a,** The long-term total

360 column time series of HCl at Jungfraujoch (running average with a 3-yr integration

361 length, step of 1 month; in red, left scale, in molecules per cm<sup>2</sup>) and the global total

362 tropospheric chlorine volume mixing ratio (blue curve, right scale, in parts per trillion,

363 p.p.t.). Lower panels display the running average total column time series (1997–2011) of

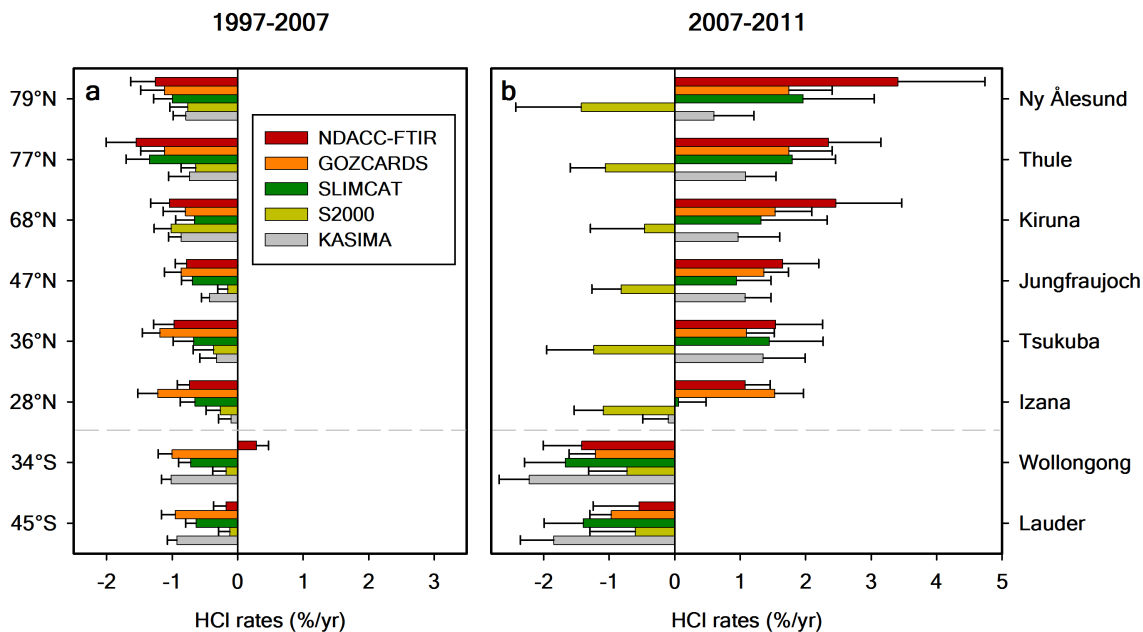
364 HCl at Ny-Ålesund (b), Jungfraujoch (c) and Lauder (d), derived from the NDACC–

365 FTIR observations and from the KASIMA run (grey). The thin red lines correspond to the

366  $\pm 2$  standard error of the mean range. The vertical dashed lines identify the occurrence of

367 the minimum total columns at the Northern Hemisphere sites, in July 2007.

368



369

370 **Extended Data Figure 2 | HCl relative rates of change at eight NDACC sites. a and b**

371 provide the rates of change (per cent per year) for the 1997–2007 (1999–2007 for Thule

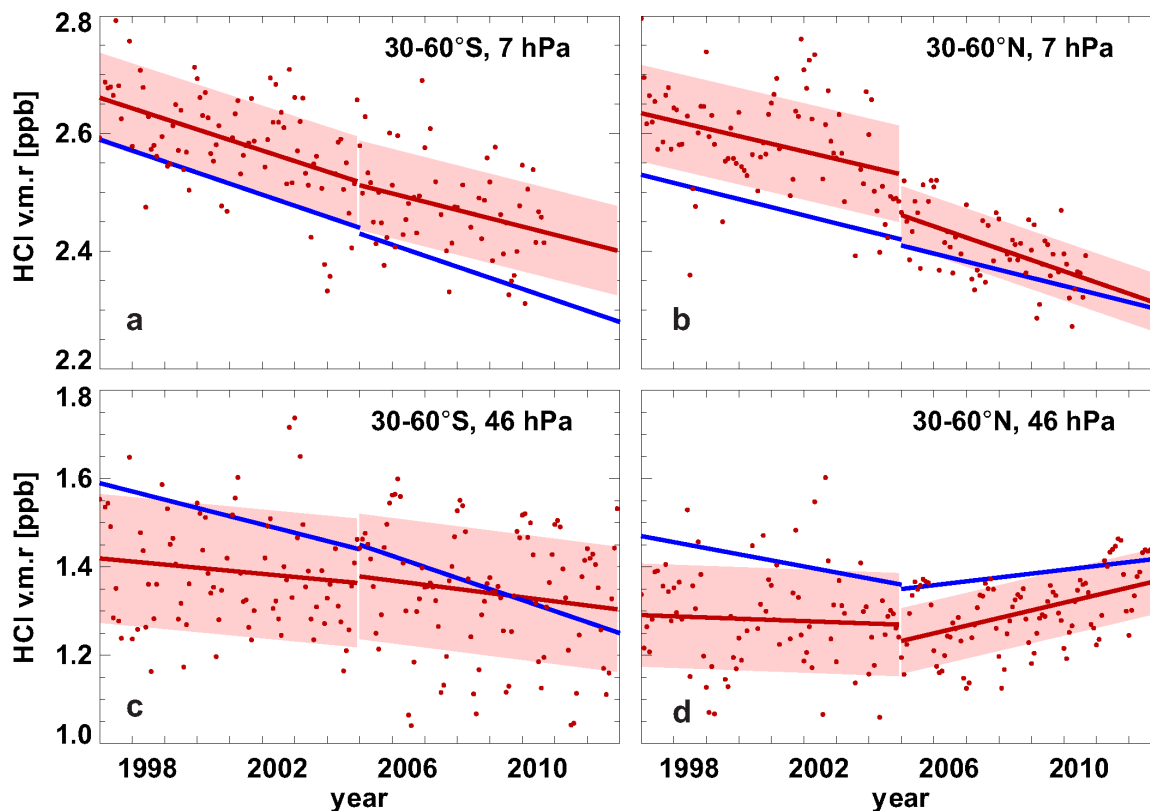
372 and Izana, 1998–2007 for Tsukuba) and 2007–2011 time periods, respectively. They

373 were derived from the FTIR and GOZCARDS observational data sets and from the

374 SLIMCAT and KASIMA simulated time series (see colour key). The error bars

375 correspond to the  $2\sigma$  level of uncertainty.

376



377

378 **Extended Data Figure 3 | Evolution of stratospheric HCl from satellite observations.**

379 Comparison of merged GOZCARDS satellite HCl observations (by HALOE, ACE-FTS

380 and Aura/MLS) with KASIMA model results for Northern and Southern Hemisphere

381 mid-latitude lower (46 hPa) and upper (7 hPa) stratosphere. GOZCARDS monthly mean

382 observations are shown as red dots. Linear fits to the GOZCARDS data and the KASIMA

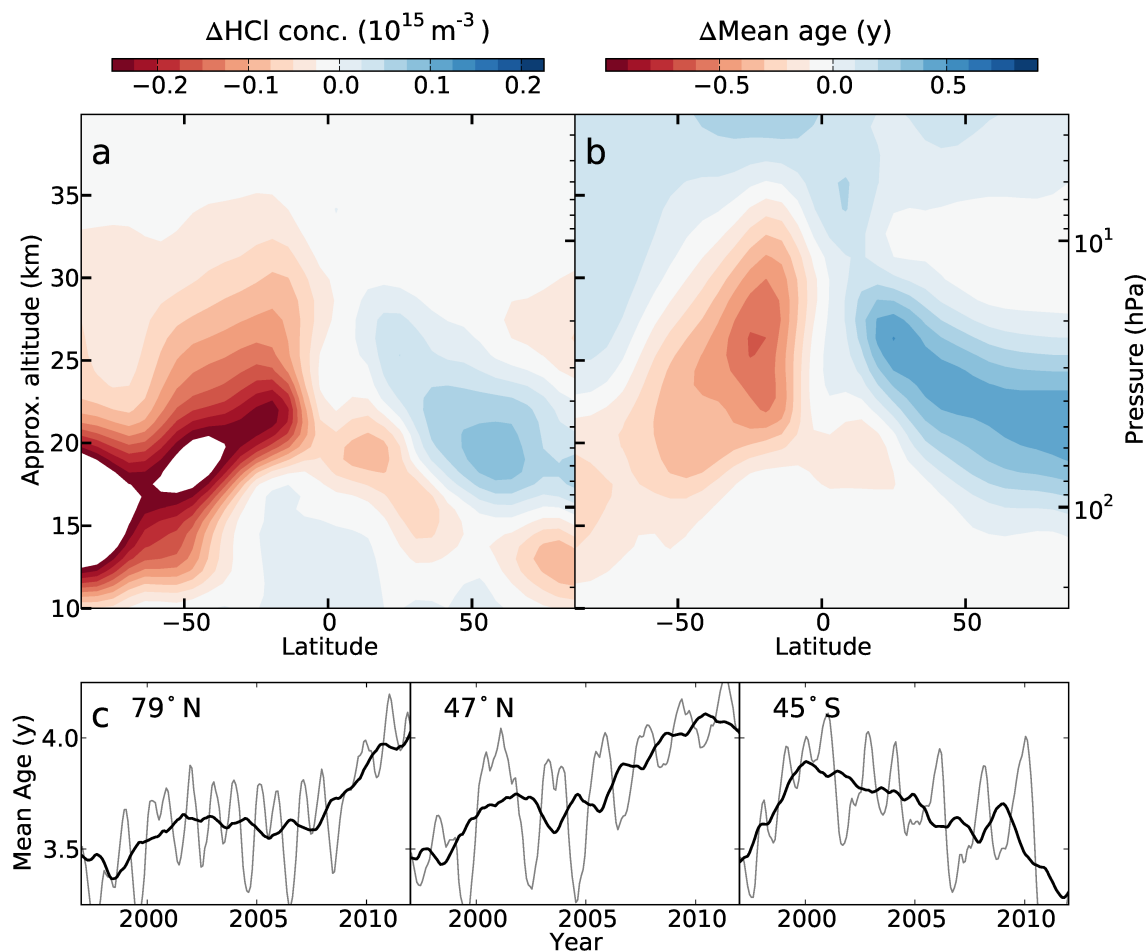
383 run are displayed as red and blue lines, respectively, for periods before and after 2005.

384 An upward trend is observed and modelled in the Northern Hemisphere lower

385 stratosphere (**d**) while HCl is decreasing in the southern and northern upper stratosphere386 (**a, b**); volume mixing ratio (vmr) in parts per billion (p.p.b.).

387





388

389 **Extended Data Figure 4 | Spatial distribution of the HCl concentration and age-of-**  
390 **air changes.** Mean differences of the HCl concentration (a) and age-of-air (b) between  
391 2010/11 and 2005/06, as a function of altitude and latitude, derived from the KASIMA  
392 model simulation. c, Running averages of the mean age-of-air at 50 hPa (thick/thin curve,  
393 integration length of 36/6 months), at the same sites as in Fig. 1 (time series at 79°N/45°S  
394 have been shifted vertically by  $-0.75/-0.50$  yr). Comparison with age-of-air time series  
395 derived from SLIMCAT (see Fig. 4c) indicates that KASIMA provides higher absolute  
396 values of mean age-of-air. Note that the upper boundary of KASIMA is at 120 km,  
397 yielding higher mean ages, compared to SLIMCAT (upper boundary 60 km).